



Drop strength measurement of green pellet based on drop-rebound mechanism

Jie Lei^{1,2} · Xu Gao¹ · Jing-shu An¹ · Guang-da Bao¹ · Yu-qi Kong¹ · Hong-ming Long^{1,2}

Received: 7 September 2022 / Revised: 2 January 2023 / Accepted: 6 January 2023 / Published online: 7 June 2023
© China Iron and Steel Research Institute Group Co., Ltd. 2023

Abstract

The construction of blast furnace charge structure based on pellet and the development of short process from non-blast furnace to electric furnace will be an efficient way to accomplish “carbon peak, carbon neutral”. Since drop strength is one of the most crucial quality indexes for green pellet, the crack detection in the collision process is an indispensable segment; however, the present crack determination is basically completed manually. Due to a series of problems including high labor intensity and poor detection conditions, it is urgent to develop an accurate, convenient and fast standardized method for drop strength detection. In view of the above issues, combined with plenty of experimental studies, it is found that whether rebound occurs after the collision of green ball can be used as the basis for judging if there are cracks on the surface, and the mechanism of this segment is explained by the energy conversion of collision process that the plastic deformation of the collision is a cumulative process. Each collision will cause a slight displacement of the iron ore particles; until the cumulative displacement exceeds the binding force between the particles, they will slip in a large range, that is, cracks will occur. The drop strength can be detected based on the drop-rebound mechanism determining crack generation during collision process by high-speed cameras, and the method is fully applicable to oxidized pellets with particle size of 8–16 mm though various pellet plasticities and masses increase the difficulty of bounce height monitoring. Based on the drop-rebound mechanism of green pellet, three methods for automatically detecting the drop strength are proposed, which are high-speed camera, photoelectric sensor and pressure sensor methods.

Keywords Green pellet · Drop strength · Collision · Rebound · Crack

1 Introduction

Powder materials, including iron ore and solid waste, will cause undesirable consequences when used directly in metal smelting, such as decreasing reactor permeability, increasing furnace pressure, deteriorating reduction kinetics and even resulting in malignant safety accidents. Pelletizing is one of the most essential methods to make powder materials into qualified products of which physical properties and chemical composition meet subsequent

process. Oxidized pellets and carbon-containing pellets are the indispensable charge materials for both blast and non-blast furnace ironmaking process including MIDREX, HYL, COREX and rotary hearth furnace. Considering the good mechanical and metallurgical properties of pellet, such as uniform particle size, high cold strength, high iron grade, low energy consumption and low pollutant emission [1], the construction of blast furnace charge structure based on pellet and the development of short process from non-blast furnace to electric furnace will be an effective way to achieve “carbon peaking and carbon neutrality” [2, 3].

Most of the powder materials are agglomerated into spherical, hemispherical, ellipsoidal or pillow-shaped pellets with suitable particle size by disk granulator or twin-roller machine and then transfer to the follow-up processes by belt conveyor successively. Due to the altitude intercept of the belts, it is inevitable that the green pellet (pellets without high-temperature roasting) will fall and collide

✉ Hong-ming Long
yafhm@126.com

¹ School of Metallurgical Engineering, Anhui University of Technology, Ma’anshan 243032, Anhui, China

² Key Laboratory of Metallurgical Emission Reduction and Resource Comprehensive Utilization, Anhui University of Technology, Ma’anshan 243032, Anhui, China

several times with different heights during the transport. If green pellet is not strong enough to resist the transient impact, it will break directly or form “internal injuries” to break gradually in subsequent process, which will significantly reduce the efficiency and even affect smooth production [4, 5]. In production, the drop strength of green pellets is defined as the drop number of pellets that dropped freely from a fixed height onto a non-deformed steel plate (generally a 10-mm-thick steel plate) repeatedly until break or produce cracks. Different companies and processes have different standards for the drop height, and the common ones are 0.5, 1.0 and even 1.5 m.

At present, the drop strength measurement of green pellet is basically done manually. The inspectors repeatedly bend down and squat to count the drop number of green pellet until the crack appears, which is observed in pellet surface by naked eye; thus, the whole process is laborious, tedious and subjective. In addition to factors like poor light, high requirements on the eye intensity and operator responsibility are put forward; therefore, the development of standardized automatic detection method for the drop strength of green pellets makes all the difference. Several studies [6–9] partially reduced the labor intensity and improved the inspection accuracy through equipment development and mechanical modification; however, they mainly focused on the standardization of factors including drop height and bottom steel plate, and the key problems of cracks observation and drop number determination are still hard to be resolved fundamentally. The rapid development of image recognition technology provides solutions to these problems. The typical network models, like fully convolutional network, U-net, SegNet, etc., are introduced into crack detection [10], while the image recognition is used to observe the pellet grain size and determine the grain size distribution [11]. Furthermore, the method of image recognition combined with depth network is proposed to observe the surface cracks during the falling of green pellet, and the advantages and limitations of depth network in particle crack detection are also analyzed [12].

The method of image recognition combined with the depth network can solve the observation problem of surface cracks of green pellet, thus providing a basis for the determination of the drop number. However, due to the complexity of cracks and the difficulty of complete acquisition of green pellet surface images and the moisture or light limitations, a series of problems need to be solved for the application of this method in drop strength detection. In this paper, based on the drop-rebound characteristics of the ball, three detection methods are proposed to determine the drop strength of pellet, and the mechanism of the method is explained theoretically.

2 Analysis for collision process of green pellet falling

2.1 Force between particles in green pellet

The pelletized material exists in the form of particle agglomerates under the action of water and binder. The bonding between particles mainly relies on the coupling effect of van der Waals force, electrostatic force, mechanical interlocking force, capillary force generated by capillary water and viscous force provided by binder to overcome the self-gravity. Among them, van der Waals force, capillary force, viscous force and mechanical interlocking force are conducive to particle agglomeration, while electrostatic force and gravity hinder particle agglomeration. The mechanical interlocking force is mainly related to the particle morphology, which is not discussed here. The van der Waals force between particles is the set of forces between multiple atoms or molecules. Assuming that the particle shape is approximately spherical and the interaction between all atoms or molecules in the particle is additive, the van der Waals force F_{van} between particles can be calculated according to Eq. (1) [13, 14].

$$F_{\text{van}} = \frac{AR_1R_2}{6S^2(R_1 + R_2)} \quad (1)$$

where R_1 and R_2 are the particle radius, m; A is the particle Hamaker constant in vacuum, N m; and S is the distance between two spherical particles, m.

When the powder is well wetted, the water fills in the particle void to form capillary water, and then, the effect of surface tension causes capillary water to generate capillary force, of which the details are shown in Fig. 1. The capillary force F_{cap} is given as follows [15].

$$F_{\text{cap}} = 2\pi R\sigma \left[\sin\beta \sin(\beta + \theta) + \frac{R}{2} \left(\frac{1}{r_1} + \frac{1}{r_2} \right) (\sin\beta)^2 \right] \quad (2)$$

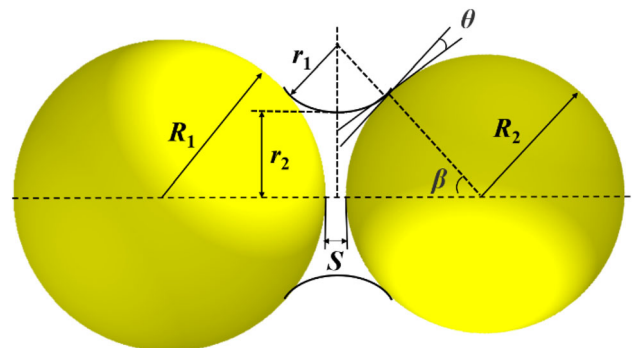


Fig. 1 Schematic diagram of liquid bridge

where σ is the liquid surface tension, N m; β is the half filling angle, ($^\circ$); θ is the contact angle, ($^\circ$); r_1 and r_2 are the radius of curvature, m; and R is the particle radius, m. r_1 and r_2 are related to θ and S .

The viscous force F_v between particles containing binder is calculated through modeling and decomposed into normal component F_{vn} and tangential component F_{vt} as follows [16–18].

$$F_{vn} = 6\pi\eta R^* v_n \frac{R^*}{S} \tag{3}$$

$$F_{vt} = \left(\frac{8}{15} \ln \frac{R}{S} + 0.9588 \right) 6\pi\eta R v_t \tag{4}$$

where η is the liquid viscosity, mPa s; v_n is the relative normal velocity, m/s; v_t is the relative tangential velocity, m/s; and R^* is the equivalent radius, m, and $R^* = 1/R_1 + 1/R_2$. When the separation distance reaches the limitation, the liquid bridge will break and lose the force. The limit separation distance (S_c) can be obtained from Eq. (5), which is related to the liquid bridge volume V .

$$S_c = (1 + 0.5\theta) V^{1/3} \tag{5}$$

From Eqs. (1)–(5), it indicates that for connected green pellet particles, van der Waals force, capillary force and viscosity force are closely related to particle size and separation distance, and these forces are decreased with the increase in the separation distance. For the oxidized pellets or carbon-containing pellets with particle size of 20–80 μm [19], the capillary force and viscous force play a dominant role in the green pellet strength.

2.2 Collision damage analysis of falling green pellet

The damage of particle agglomerates caused by collisions during production and transportation has been concerned for a long time. Rumpf [20] used free-drop test to determine the collision strength of particle agglomerates in the early stage and defined its strength mainly according to the falling height of agglomerate without obvious damage. After that, scholars [21, 25] studied the collision damage of particle agglomerates by high-speed impactor or numerical simulation and gradually paid attention to the collision damage under the adhesion of wet particles. The research of Fu et al. [26] on wet particle agglomerates has essential guiding significance for collision damage in green pellet falling process. Both oxidized pellets and carbon-containing pellets can be regarded as iron ore particle agglomerates with the moisture of 8%–15%, which is more suitable for this model.

The falling process of green pellet can be divided into two stages: loading and unloading [27, 28]. It is assumed

that the green pellet is a sphere, as shown in Fig. 2, and collides with 10-mm-thick steel plate (without deformation) after free falling from H . The instantaneous velocity reaches the maximum v_{max} when green pellet touches the steel plate, and the interaction forces are generated. The moisture of green pellet is 8%–15%, contributing to its good plasticity. During collision process, elastic and plastic deformation will occur simultaneously. Subsequently, the green pellet will decelerate from v_{max} to 0 in time t_L , which is called the loading stage. In this stage, the microstructure of the contact site between the pellet and the steel plate generates “irreversible” deformation and microcracks distributed along the warp direction randomly; at this time, slight sliding occurs between particles. Therefore, a “damage domain” propagating from outside to inside is formed on the driving face. This domain has very complex action mechanism, which has been reported in literature [29–31] and will not be introduced in detail here. The energy change of green pellet falling is shown in Eqs. (6) and (7), ignoring the air resistance.

$$mgH = \frac{1}{2} m v_{\text{max}}^2 \tag{6}$$

$$\frac{1}{2} m v_{\text{max}}^2 = mg(h_L - h_{UL}) + E_e + E_p + E_L \tag{7}$$

where m is the mass of green pellet, kg; g is the acceleration of gravity, m/s^2 ; E_e is the energy stored by elastic deformation, J; E_p is the energy consumed by plastic deformation, J; and E_L is the adhesion energy loss due to contact, J.

According to the Hertz equation, the energy consumed by plastic deformation is related to the elastic yield limit and ultimate yield velocity of the agglomerate [32]

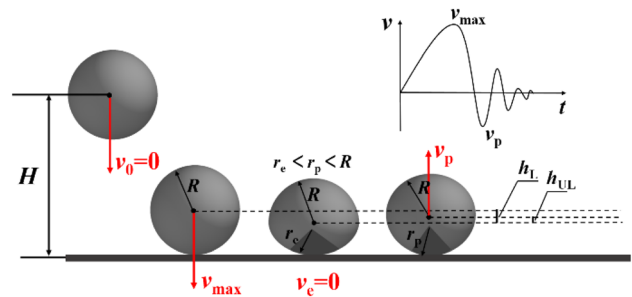


Fig. 2 Schematic diagram of falling process. H —Initial falling height, m; v —velocity of green pellet; v_0 —initial velocity of green pellet, m/s; v_{max} —maximum velocity at moment of contact with ground, m/s; v_c —final velocity of loading stage, m/s; v_p —maximum velocity during rebound, m/s; r_c —maximum damage domain radius during rebound, m/s; r_p —damage domain radius after rebound, m/s; h_L —centroid distance of pellet at time of contact with plate and at loading stage, m; h_{UL} —centroid distance of pellet at loading and unloading stage, m; t —time

$$E_p = \left[\left(\frac{1}{2}mv_{\max}^2 - E_Y/16 \right)^{1/2} - (15E_Y/16)^{1/2} \right]^2 \tag{8}$$

$$v_Y = (2\pi/3K)^2(2/5\rho)^{1/2}Y^{5/2} \tag{9}$$

where E_Y is the limiting kinetic energy, J, $E_Y = mv_Y^2/2$; Y is the elastic yield limit, N/m²; v_Y is the limiting velocity, above which plastic deformation begins to occur, and the limiting velocity is determined by the bulk material properties and is independent of particle size, m/s; K is a mechanical constant, $K = 4(\kappa_1 + \kappa_2)/3$; $\kappa_i = (1 - \nu_i^2)/\zeta_i$; ν_i is the Poisson’s ratio; ζ_i is the Young’s modulus, Pa; and ρ is the density of the particle, kg/m³.

After the loading stage, assuming that the green pellet can bounce, the elastic deformation area of green pellet will rebound. The instantaneous velocity of detachment from the steel plate reaches its maximum v_p , which is called the unloading stage. At this time, the microcracks generated in the loading stage continue to develop, which may propagate from the “damage domain” to form cracks, or may be re-closed [33, 34]. The energy changes in the unloading process are given in Eq. (10) and reorganized to get Eq. (11).

$$E_c = mg(h_L - h_{UL}) + \frac{1}{2}mv_p^2 + E_{UL} \tag{10}$$

$$\frac{1}{2}mv_p^2 = \frac{1}{2}mv_{\max}^2 - mg(2h_L - h_{UL}) - E_p - E_L - E_{UL} \tag{11}$$

where E_{UL} is the adhesion energy loss due to contact during unloading stage, J. The critical condition for the agglomerates to bounce is given in Eq. (12).

$$\frac{1}{2}mv_{\max}^2 - mg(2h_L - h_{UL}) - E_p - E_L - E_{UL} > 0 \tag{12}$$

Combined with the analysis of Eqs. (10)–(12), it can be concluded that whether the agglomerates can bounce after the collision process with the steel plate depends on the energy variation, especially the energy direction of the loading stage. Scholars have studied the conditions of particle agglomerates bounce after falling. For example, Thornton et al. [35–37] believed that it is related to the incident velocity of the agglomerates. For the green pellet drop from the same height repeatedly, the incident velocity of each falling process keeps the same, and thus, the plastic deformation is a procedure of energy accumulation. Ignoring the pellet moisture evaporation, it can be assumed that the adhesion energy loss caused by contact during each falling process is constant, and there is little potential energy loss in the deformation process. Then, the main whereabouts of kinetic energy are the elastic potential energy stored in the elastic deformation area and the energy consumed by plastic deformation. Thereinto, the energy

consumed by plastic deformation is also related to the green pellet plasticity. With the drop strength characterized by the number of times that the green ball does free fall without breaking at the vertical distance of 0.5 m from the steel plate height, it is preliminarily inferred that when the green pellet plasticity is good that the drop strength is more than 10 times, the plastic deformation will take away a large quantity of energy, which will affect the rebound height. This inference will be verified by the following experiments.

From the drop strength detection process, it can be seen that elastic rebound occurs in the times of 0–($n - 1$) collision of green pellet. At this time, most of the initial kinetic energy is converted into the elastic potential energy, which is converted into the kinetic energy needed for rebound in turn, and the plastic deformation only consumes a small amount of energy. According to the characteristics of plastic deformation, when the energy received by the material exceeds the elastic yield limit, the material will undergo plastic deformation. For the green pellet, the main factors affecting the yield strength are van der Waals force, capillary force, viscous force and other forces among internal particles. The plastic deformation of the green pellet is a cumulative procedure; for every drop-rebound process, slight slippage will occur between the particles, and the distance of slippage is also continuously accumulated. However, it still does not get rid of the restriction of the force between the particles; thus, the energy consumed by plastic deformation is limited, and the green pellet will have no obvious cracks. According to Eqs. (1)–(4) and relevant parameters in Table 1, the relationship between the strength of van der Waals force, capillary force and viscous force and the distance among particles was calculated. As shown in Fig. 3, the three forces decreased with the increase in the separation distance, and therefore, the

Table 1 Correlation parameters of force between iron ore particles

Physical parameter	Value	Physical parameter	Value
Volume density of iron concentrate/(g cm ⁻³)	3.40	Hamaker constant/(N m)	3.8×10^{-20} (water) [38]
Particle diameter/m	74×10^{-6}	Liquid surface tension/(N m ⁻¹)	0.072 (25 °C, water) [19]
Half angle of connecting bridge/(°)	30	Separation velocity/(cm s ⁻¹)	1.67×10^{-2} [38]
Viscosity of connecting bridge/(Pa s)	0.001		

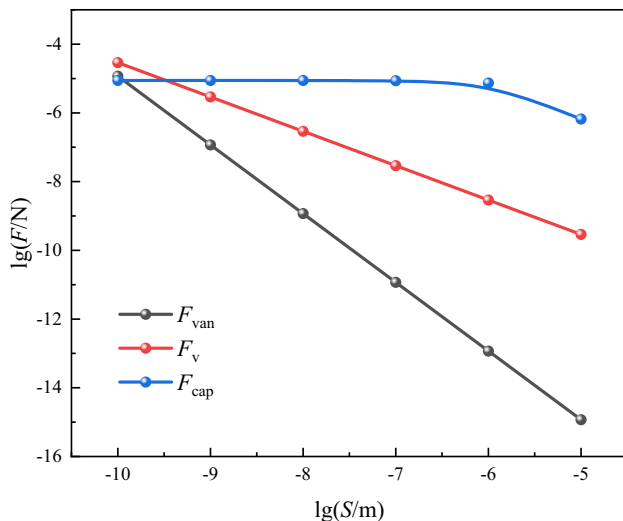


Fig. 3 Relationship between van der Waals force, capillary force, viscosity force and particle spacing

bonding force between particles is weakened gradually with the continuous collision.

When the green pellet just no longer rebounds at the times of n collision, obvious cracks and even ruptures appear on the green pellet surface. The process is actually the expansion of plastic deformation area, when the agglomeration forces such as van der Waals force, capillary force and viscous force are less than the electrostatic repulsion and gravity. There is a large range of slip between iron ore particles, and even some particles directly get rid of the bulk ejection, and plastic deformation takes away almost all energy.

3 Drop strength determination of green pellet based on drop-rebound mechanism

3.1 Experimental procedure

In this paper, the drop-rebound characteristics of oxidized pellets were studied. The experimental process mainly included three parts: green pellet preparation, drop strength detection and video capture during collision process. The iron concentrate and bentonite were mixed in proportion and ground in a $\phi 300 \text{ mm} \times 400 \text{ mm}$ mill for 30 min. The moisture content was 7.5%, and the filling rate of the mill was 20%. The mixture was taken out to pelletize after grinding. The green pellet was prepared in a disk pelletizer of 1000 mm in diameter and 200 mm in side height. The inclination angle of the equipment was adjustable in the range of 45° – 47° , and the rotational speed was 23 r/min. The pelletizing time was 15 min. The moisture of green pellet was controlled in the range of 8.0%–10.0%

according to the plastic requirement. The artificial feeding and watering were used in the pelletizing. The cue ball was prepared in 2 min and then grew up to the target size in 10 min.

In order to eliminate the interference of green pellet particle size on drop strength, qualified green pellets with diameter of d – $(d + 1)$ mm were selected for drop strength detection according to the standard method. The selected qualified pellets were stored by preservative film in the shade to prevent moisture escaping. The drop strength of green pellets was tested according to the following steps.

- (1) Pellets dropped freely from the height of 0.5 m onto the steel plate of 10 mm in thickness.
- (2) After falling, carefully observe whether cracks or ruptures were produced on the surface of the pellets.
- (3) If the cracks or breakage appeared on the surface of the pellet, the inspection is finished; contrarily, repeat steps (1) and (2).
- (4) When the crack or breakage occurred after the pellet dropped at the times of n , then the drop strength P_i (times) of a single pellet is as follows.

$$P_i = (n-1) \quad (13)$$

The average drop strength of 10 pellets was used as the drop strength Q (times) of the pellets batch. If the drop strength of a single pellet appears to be significantly different from other pellets, the additional measurement will be carried out.

$$Q = \frac{\sum_{i=1}^{10} P_i}{10} \quad (14)$$

A high-speed camera was installed to record the contact process between the green pellet and the steel plate in real time, as shown in Fig. 4, and the drop number of falling pellets was determined by whether the green pellet bounced through later image processing. The ratio of bentonite was adjusted by 0.6%, 1.2%, 1.8%, 2.4% and 3.0% successively to regulate the plasticity of the green pellet. Green pellets with size of 8–9, 12–13 and 15–16 mm were selected for drop-collision process detection. The influence of the plasticity and mass of green pellet on the collision rebound process was studied, and under each working condition, the drop strength was detected three times repeatedly.

3.2 Results and discussion

The experimental results are shown in Table 2 and Fig. 5. In Table 2, due to the narrow selection range of green pellet size, the drop strength had slight fluctuations. With the increase in bentonite addition, the drop number

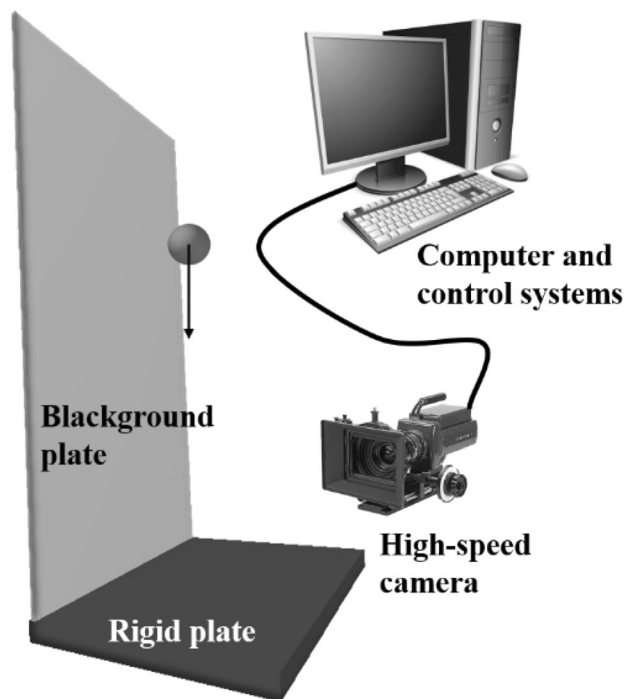


Fig. 4 Determination for drop strength of green pellets based on high-speed camera image recognition

Table 2 Comparison of drop strength testing of green pellets

No.	Bentonite ratio/%	Green pellet diameter/mm	Drop strength/times	
			Traditional method	Drop-rebound method
1	0.6	12–13	1.4, 1.3, 1.5	1.4, 1.3, 1.3
2	1.2	12–13	3.2, 3.4, 3.2	2.8, 3.3, 3.1
3	1.8	12–13	6.8, 6.9, 6.0	6.7, 6.7, 6.0
4	2.4	12–13	9.2, 9.5, 9.8	9.0, 9.5, 9.7
5	3.0	12–13	14.2, 14.5, 14.5	14.1, 14.2, 14.4
6	1.8	12–13	6.2, 6.8, 6.7	6.2, 6.7, 6.7
7	1.8	15–16	6.1, 6.5, 6.0	6.1, 6.4, 6.0

increased, and the green pellets plasticity enhanced gradually. As shown in Fig. 5a–i, the green pellet, with diameter of 12–13 mm and drop strength of 3.0 times (0.5 m), rebounded after the first three collisions on the steel plate, and the final rebound height remained 10.8 mm though it decreased gradually. After the last drop test, the green pellet was no longer bounced and there were small fragments ejected. As shown in Fig. 5j–l, the traditional detection method considers this time as the end of detection, that is, the end of detection can be judged by whether

the green pellet rebounds during the falling collision process.

Further analysis shows that the drop strength measured by the drop-rebound method is generally less than or equal to the results of traditional method, mainly because it is difficult to discover the hidden micro cracks by naked eye in the traditional method. Therefore, the proposed method in this paper is used with higher accuracy.

According to the above analysis, the plasticity and mass of the green pellet may affect the energy consumed by plastic deformation, thereby affecting the rebound height and even the possibility that the unwounded green pellet will not rebound, and ultimately affecting the detection accuracy. Figure 6 shows the first, reciprocal third, reciprocal second rebound and the last drop-collision process of green pellets with different plasticities and masses (by different sizes). The comparative analysis shows that the plasticity and mass of green pellet have a great influence on the rebound height after collision, and the bounce height is substantially lower as the plasticity or weight increases. When the particle size of green pellet was 15–16 mm and the drop number was 14.0 times, the last rebound height was only 5.2 mm. The decrease in rebound height will increase the difficulty of identification; however, the general particle size of oxidized pellets is 8–16 mm, and the drop number is generally 5–10 times, which are lower than the detection limit of this method. Subsequently, spheroid-shaped pellets with a size of 15 mm × 25 mm × 32 mm were prepared by briquetting process. Since it was observed from the last row of Fig. 6d that the pellets shape had no significant influence on the application of the drop-rebound method, it can be concluded that the drop strength detection method based on the drop-rebound mechanism was applicable to almost all pellets in the metallurgical industry.

4 Detection method of drop strength of green pellet based on drop-rebound mechanism

4.1 High-speed camera method

High-speed camera is a device that can capture motion images at a frame rate of less than 1/1000 s exposure or more than 250 frame/s, which is used to record fast-moving objects as photographic images onto the storage medium. Most of the drop strength detection of green pellet is based on 0.5 m height, and the time for green pellet to complete the drop-rebound process is about 0.35 s. The high-speed camera is fully capable of satisfying the determination of whether the green pellet rebounds, and laboratory tests have verified this. As shown in Fig. 4, a

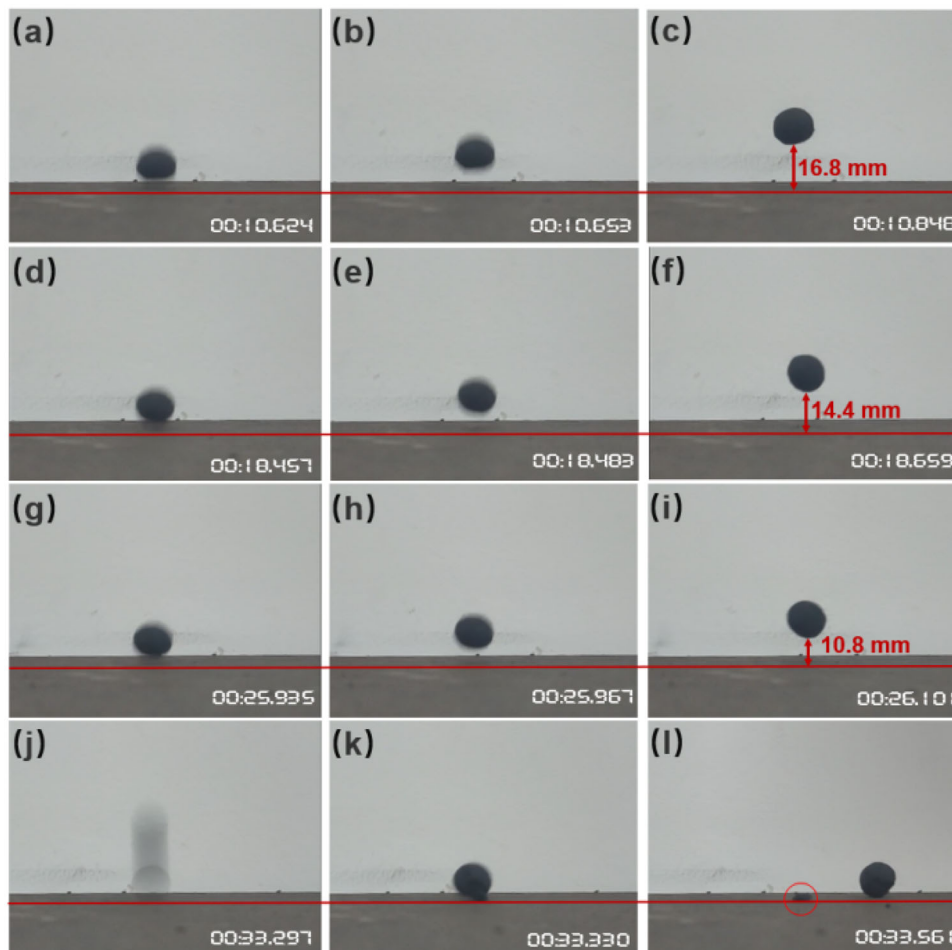


Fig. 5 Schematic diagram of green pellet drop-collision process ($d = 12\text{--}13$ mm, $P_t = 3.0$ times). **a, d, g, j** Before contact between green pellet and steel plate; **b, e, h, k** after collision between green pellet and steel plate; **c, f, i, l** highest point of green pellet rebound

high-speed camera is used to record the drop-rebound process, and whether the green pellet bounces or not is used as the basis for determining the drop number by computer and image recognition, which can accurately detect the drop strength of the green pellet, where the background plate is mainly used for light supplementation.

4.2 Photoelectric sensor method

Photoelectric sensor is usually composed of optical transmitter, optical original circuit and signal conversion circuit. The optical transmitter sends out optical signals containing information in various ways. When a particular test object passes through the photoelectric sensor, the optical circuit is blocked by the test object, and the receiver immediately responds and sends control signals at this time. Based on this feature, the use of green pellets in the drop-rebound process to determine whether the optical circuit is blocked or not and then detect the drop number of green pellet. According to the relevant literature, the contact time

between the green pellet and the steel plate is about 0.2–0.7 ms [39, 40], and the response time of the current advanced photoelectric sensor can be as low as 0.02 ms, which can fully meet the requirements. As shown in Fig. 7, considering the limited rebound height of the green pellet drop-rebound process, the optical transmitter should be arranged as close to the bottom plate as possible to ensure that the photoelectric sensor can effectively monitor the blocked optical signal. Through the computer and control system to analyze the photoelectric signal, the automatic detection of green pellet drop strength can be achieved accurately and efficiently.

4.3 Pressure sensor method

According to the analysis of Rogers and Reed [41] on the drop-rebound process of particle agglomeration force, the force F_N exerted on the contact surface by green pellet includes the force F_e acting on the elastic region and the force F_p acting on the plastic deformation region:

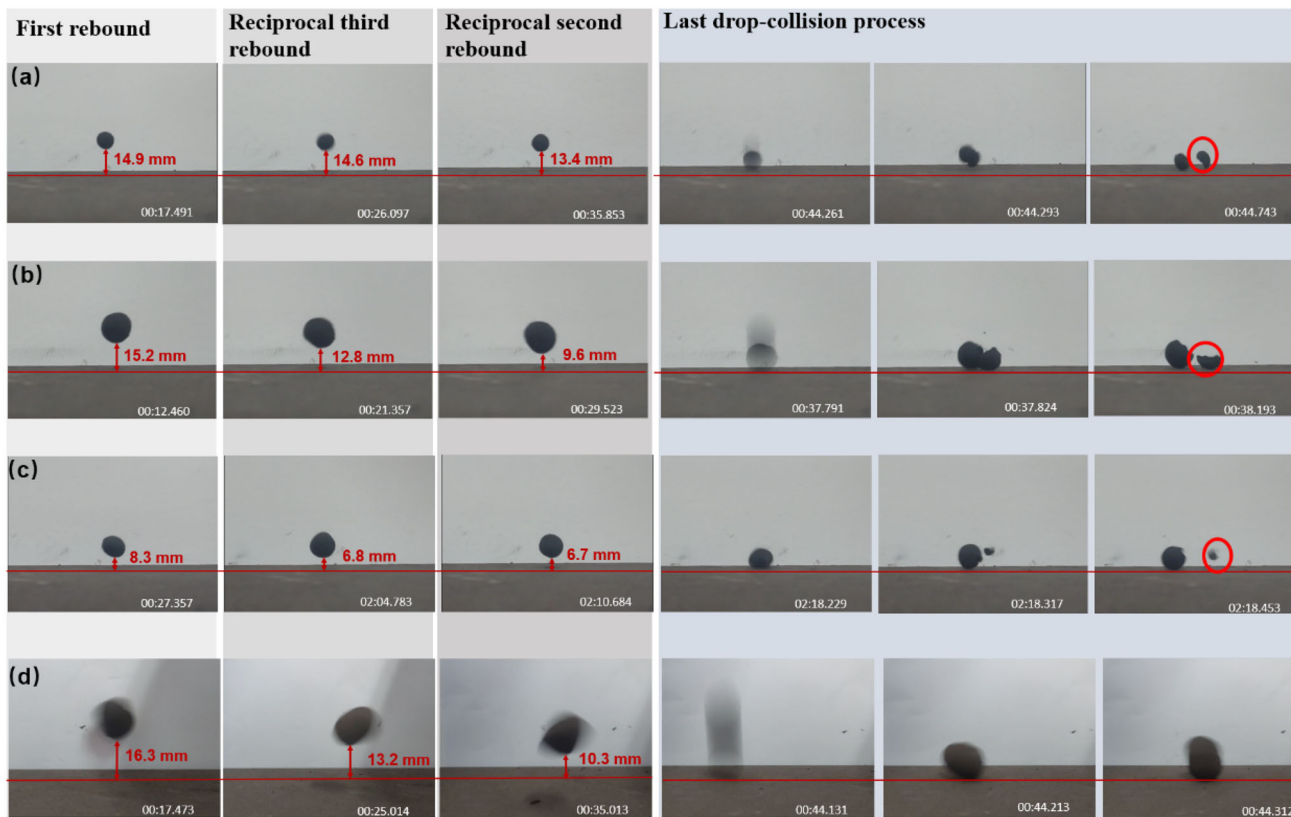


Fig. 6 Effect of plasticity and particle size of green pellet on drop-collision process. **a** $d = 12\text{--}13$ mm, $P_i = 14.0$ times; **b** $d = 15\text{--}16$ mm, $P_i = 3.0$ times; **c** $d = 15\text{--}16$ mm, $P_i = 14.0$ times; **d** $15\text{ mm} \times 25\text{ mm} \times 32\text{ mm}$, ellipsoidal, $P_i = 3.0$ times

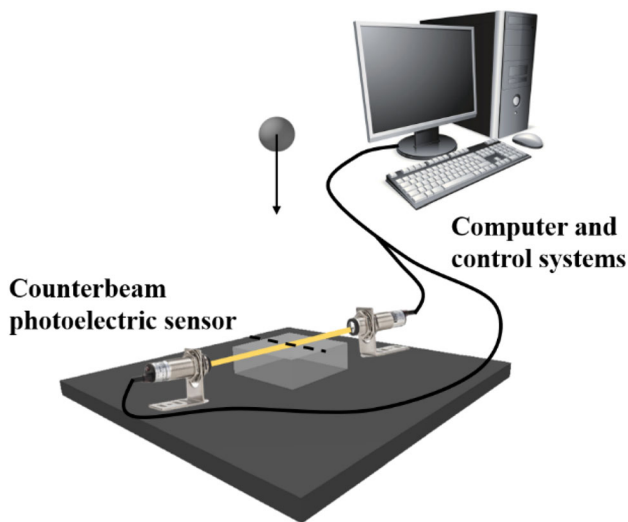


Fig. 7 Determination for drop strength of green pellets based on high-speed camera image

$$F_N = F_e + F_p \tag{15}$$

where $F_e = (R^{1/2}K)^{2/5}(5E_Y/2)^{3/5}$; $F_p = \pi r_p^2 Y$; and r_p is the contact radius of plastic deformation zone, m, $r_p = 3K[(15/16)E_Y E_P]^{1/4} / [(\pi Y)^{3/2} R^{1/2}]$.

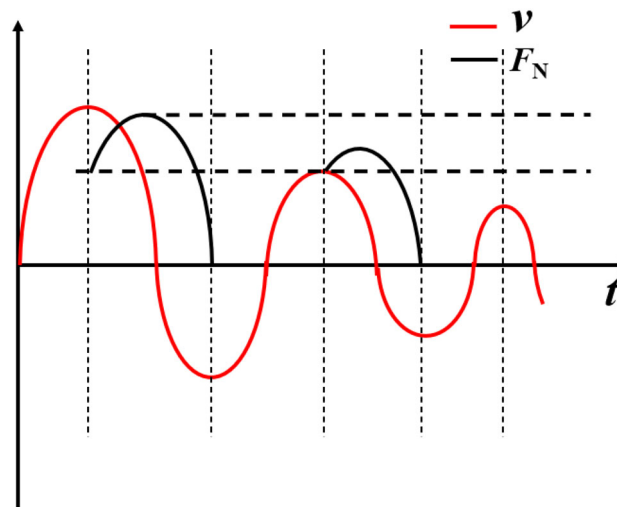


Fig. 8 Hypothetical curves of velocity and force between falling green pellet and steel plate during collision

As shown in Fig. 8, it suggests that in the loading process, F_N gradually increases with the decrease in the green pellet speed, and the pressure reaches the maximum when the speed decelerates to 0. After the green pellet enters the unloading stage, the pressure gradually decreases from the peak to 0, when the green pellet is just out of contact with

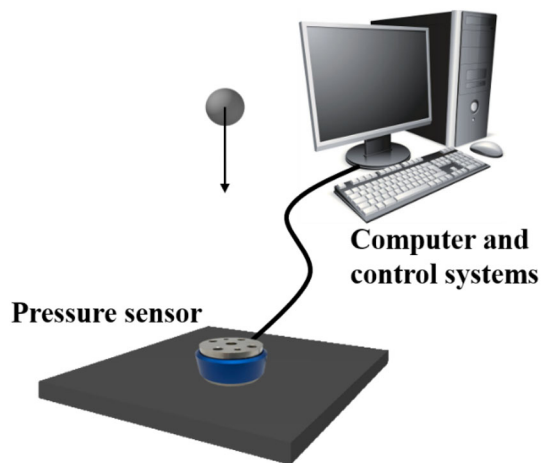


Fig. 9 Determination for drop strength of green pellet based on pressure sensor

the steel plate. The above process is circulated when the green pellet is dropped repeatedly. Therefore, the drop strength detection of green pellet can be realized by the high-sensitive pressure sensor. As shown in Fig. 9, the high-pressure sensor will record the pressure change during the green pellet drop-rebound process. If the pressure increases periodically and then decreases to 0, it will be determined that the green pellet can be bounced; contrarily, it will be determined that the green pellet cannot be bounced with cracks or breakage appearing in the surface.

From the cost point of view, the photoelectric sensor has the greatest advantage and is easy to maintenance, while the pressure sensor method requires the use of high sensitivity sensor with relatively high price, and the high cost of high-speed camera equipment is also well known. From the perspective of measurement accuracy, the high-speed camera is the best, since the storage of the camera determines its function of re-proofreading. More accurate test results can be obtained by multiple comparisons through image processing and other technical means. The photoelectric sensor needs to set the corresponding photosensitive position according to the pellets size which is various with different pellets in the actual detection, and thus, it will cause some errors. For pressure sensors, the accuracy of the measurement depends on the precision of the equipment. In general, the appropriate detection method can be selected for different conditions, or the three detection methods can be used in combination.

5 Conclusions

1. Whether the green pellet can bounce after falling and colliding with the steel plate depends on the energy change of the collision process, especially the energy

direction in the loading stage, which is an energy accumulation process. The energy mainly moves toward the elastic potential energy stored in elastic deformation region and the energy consumed by plastic deformation, and the energy consumed by plastic deformation is also related to the green pellet plasticity.

2. Elastic rebound of the green pellet occurs in the times of $0-(n-1)$ collision process. Most of the initial kinetic energy is converted into elastic potential energy, and plastic deformation only consumes a small part of energy. Obvious cracks or even ruptures appear on the pellet surface when it just stops rebound at the times of n collision. This is actually the expansion of the plastic deformation area, where a wide range of slip happens between iron ore particles and even some particles directly peel off from the body, and the plastic deformation takes away almost all the energy.
3. Using high-speed cameras to monitor the collision process of dropped green pellets, the drop strength can be detected based on the drop-rebound mechanism determining crack generation. Though various pellet plasticity and mass increase the difficulty of bounce height monitoring, the method is still fully applicable to oxidized pellets with particle size of 8–16 mm.
4. Based on the drop-rebound mechanism of collision process of green pellet, three methods were proposed to detect the drop strength of green pellet by high-speed camera, photoelectric sensor and pressure sensor, which will provide more guidance and options for industrial applications. The appropriate detection method can be selected for different conditions, or the three detection methods can be used in combination.

Acknowledgements The authors would like to deeply appreciate the fund support from the Excellent Youth Foundation of Anhui Scientific Committee (2208085J19).

Declarations

Conflict of interest The authors declare no potential conflict of interest.

References

- [1] C.S. Hu, *China Metallurgy* 31 (2021) No. 6, 54–60.
- [2] Y. Xing, W.B. Zhang, W. Su, W. Wen, X.J. Zhao, J.X. Yu, *J. Eng. Sci.* 43 (2021) 1–9.
- [3] Q. Yue, X.C. Chai, Y.J. Zhang, Q. Wang, H.M. Wang, F. Zhao, W. Ji, Y.Q. Lu, *Environ. Dev. Sustain.* 25 (2023) 4065–4085.
- [4] Y.N. Lu, S.L. Wu, H. Zhou, L.M. Ma, Z.J. Liu, Y. Wang, *ISIJ Int.* 61 (2021) 2211–2219.

- [5] X.H. Fan, G.M. Yang, X.L. Chen, X.N. He, X.X. Huang, L. Gao, *Powder Technol.* 267 (2014) 11–17.
- [6] J.X. Li, D.W. Xiang, R.F. Wei, A detection equipment for dropping strength of green pellets in motion, 112816170A, China, 2011.
- [7] J. Qin, G.G. Liu, J.L. Qi, A pellet falling strength test device and test method, 110702539A, China, 2020.
- [8] J.X. Li, D.W. Xiang, A device of metallurgical green pellet falling strength detection and application method, 106018073A, China, 2016.
- [9] J.Y. Li, Z.W. Liu, F. Geng, A device of rotary pellet falling strength detection and application method, 207263558U, China, 2018.
- [10] H.Y. Duan, J.J. Wei, L. Qi, X.D. Wang, Y. Liu, M. Yao, *Steel Res. Int.* 92 (2021) 2100168.
- [11] X.Y. Liu, C.G. Mao, W. Sun, X. Wu, *ISIJ Int.* 58 (2018) 2088–2094.
- [12] S.Y. Zhou, X.Y. Liu, Y.R. Chen, X.H. Sun, *ISIJ Int.* 62 (2022) 1694–1704.
- [13] K.L. Mittal, *Particles on surfaces*, Plenum Press, New York, USA, 1988.
- [14] J.N. Israelachvili, *Intermolecular and surface forces*, Academic Press, London, UK, 1991.
- [15] F.M. Orr, L.E. Scriven, A.P. Rivas, *J. Fluid Mech.* 67 (1975) 723–742.
- [16] R.H. Davis, J.M. Serayssol, E.J. Hinch, *J. Fluid Mech.* 163 (1986) 479–497.
- [17] G. Lian, M.J. Adams, C. Thornton, *J. Fluid Mech.* 311 (1996) 141–152.
- [18] A.J. Goldman, R.G. Cox, H. Brenner, *Chem. Eng. Sci.* 22 (1967) 653–660.
- [19] Q.M. Meng, Research on mechanical properties of carbon-bearing pellets and modification of its thermal strength, Anhui University of Technology, Anhui, China, 2019.
- [20] H. Rumpf, The strength of granules and agglomerates, in: *Agglomeration-first International Symposium on Agglomeration*, 1962, pp. 379–418.
- [21] A.V. Potapov, C.S. Campbell, *Powder Technol.* 81 (1994) 207–216.
- [22] M.J. Adams, M.A. Mullier, J.P.K. Seville, *Powder Technol.* 78 (1994) 5–13.
- [23] A. Samimi, M. Ghadiri, R. Boerefijn, A. Groot, R. Kohlus, *Powder Technol.* 130 (2003) 428–435.
- [24] G.Q. Wu, D.Y. Lin, H.W. Wang, L.Q. Liu, *J. Vis.* 25 (2022) 31–45.
- [25] F. Kun, H.J. Herrmann, *Comput. Methods Appl. Mech. Engrg.* 138 (1996) 3–18.
- [26] J. Fu, M.J. Adams, G.K. Reynolds, A.D. Salman, M.J. Hounslow, *Powder Technol.* 140 (2004) 248–257.
- [27] L.F. Liu, *Adv. Mech.* 36 (2006) No. 4, 599–610.
- [28] T. Trung Vo, S. Nezamabadi, P. Mutabaruka, J.Y. Delenne, E. Izard, R. Pelleng, F. Radjai, *Eur. Phys. J. E* 42 (2019) 127.
- [29] M.I. Hossain, R.A. Tarefder, *Constr. Build. Mater.* 49 (2013) 536–546.
- [30] J. Xiao, W. Li, D.J. Corr, S.P. Shah, *Cem. Concr. Res.* 52 (2013) 82–99.
- [31] S. Oller, E. Oñate, J. Oliver, J. Lubliner, *Eng. Fract. Mech.* 35 (1990) 219–231.
- [32] J.G.A. Bitter, *Wear* 6 (1963) 169–190.
- [33] S. Wall, W. John, H.C. Wang, S.L. Goren, *Aerosol Sci. Technol.* 12 (1990) 926–946.
- [34] L. Kogut, I. Etsion, *J. Colloid. Interface Sci.* 261 (2003) 372–378.
- [35] K.D. Kafui, C. Thornton, in: C. Thornton (Eds.), *Powders & Grains 93*, Birmingham, UK, 1993, pp. 401–406.
- [36] C. Thornton, K.K. Yin, M.J. Adams, *J. Phys. D Appl. Phys.* 29 (1996) 424.
- [37] C. Thornton, M.T. Ciomocos, M.J. Adams, *Powder Technol.* 140 (2004) 258–267.
- [38] T. Jiang, *Iron ore agglomeration*, Central South University, Hunan, China, 2016.
- [39] I.V. Oladyshkin, A.A. Oladyshkina, *Phys. Educ.* 52 (2017) 013006.
- [40] R. Cross, *Phys. Educ.* 52 (2017) 033002.
- [41] L.N. Rogers, J. Reed, *J. Phys. D Appl. Phys.* 17 (1984) 677.

Springer Nature or its licensor (e.g. a society or other partner) holds exclusive rights to this article under a publishing agreement with the author(s) or other rightsholder(s); author self-archiving of the accepted manuscript version of this article is solely governed by the terms of such publishing agreement and applicable law.